Space-Charge Wave Considerations in MIS Waveguide Analysis

Keli Han, *Student Member, IEEE*, and Thomas T. Y. Wong, *Member, IEEE*

Abstract—**A transport-based small-signal analysis of the fundamental mode of propagation in a metal–insulator–semiconductor (MIS) waveguide is presented. The formulation incorporates the full set of Maxwell's equations and the equations of motion of the carriers based on a drift-diffusion model, providing a quantitative description of the space-charge wave induced at the surface of the semiconductor. Effects of an external dc bias on the propagation characteristics are also accounted for. Numerical solutions to the system of equations for a waveguide with typical material parameters and dimensions are obtained using an iterative algorithm. Results indicate that the transverse component of the electric field in the semiconductor is strongly influenced by the screening effect of the charge carriers, whereas the longitudinal component is governed mainly by energy dissipation arising from the conduction current. The presented formulation can also find application for other multilayer structures which support a strong interaction between the electromagnetic field and the charge carriers.**

I. Introduction

THE metal–insulator–semiconductor (MIS) waveguide, being one of the most elementary configurations representative of the multilayer arrangement found in monolithic microwave integrated circuits, has been of fundamental interest since the early stage of investigation on the application of planar technology for work at microwave frequencies. Interest in the MIS structure arose not only from its role as an interconnecting element, but also from its ability to respond to an external bias, resulting in a controllable phase delay. After the early work of Hyltin [1], experimental and theoretical studies with various aspects of emphasis were carried out [2]–[13]. It has been well established that the resistivity–frequency plane can be divided into three regions: the dissipative dielectric region, the slow-wave region, and the skin-effect region. Recent quasi-TEM analysis on coplanar structure has made the incorporation of metallic conductor losses in the analysis possible and has provided a physical basis for the construction of equivalent circuits [14].

While it is possible to describe the reduction of the electric field intensity in a semiconductor and the energy dissipation of a guided wave in an MIS structure by characterizing the semiconductor with a uniform conductivity, an additional degree of freedom must be introduced in order to describe the behavior of the semiconductor as a solid-state plasma, the accumulation and depletion of carriers resulting from external bias being a typical example. For a guided wave in an MIS structure, the screening effect of the carriers prohibits the field from penetrating deep into the semiconductor, in addition to that caused by attenuation effect arising from energy dissipation. The former is found in both static (*CV* characteristic of an MOS capacitor) and dynamic cases, whereas the latter is strictly of dynamic relevance. The merits of a transport-based analysis have been demonstrated by its application to wide microstrips over doped semiconductor layers with either ohmic or Schottky contacts [15]. Carrier transport consideration has played a central role in the analysis of microwave semiconductor devices, a recent example being the application of the field-transport formulation to the analysis of a GaAs double-drift IMPATT diode [16].

In this paper, a theoretical investigation of the fundamental mode of propagation in a biased parallel-plate MIS structure employing the complete set of Maxwell's equations and the equations of motion of the carriers is presented. The charge densities and the velocities of the carriers, although constrained by the continuity equations, are each considered as a function of position and time. The coupling of the carrier motion to the electromagnetic wave gives rise to a space-charge wave guided along the surface of the semiconductor. It is noteworthy that this kind of wave–carrier interaction has been considered extensively in the analysis of microwave tubes. However, equations describing electron ballistics appropriate for vacuum devices have to be replaced by carrier transport equations for electrons and holes in the semiconductor for the present study.

Since the conditions giving rise to hot-carrier effects of the type observed in a short-channel MOSFET are not encountered here, a drift-diffusion model for carrier transport should be adequate. An extension of the theoretical framework to incorporate energy and momentum balance of the carriers can be carried out without much difficulty. Such a formulation would be necessary when there is a large dc component of the carrier velocity, which does not arise in the present case.

In order not to complicate the problem at the onset, we assume the work functions of the materials to be such that a flat-band condition is achieved in the absence of an

Manuscript received November 15, 1990; revised March 6, 1991.
The authors are with the Department of Electrical and Computer Engineering, Illinois Institute of Technology, Chicago, IL 60616.
IEEE Log Number 9100135.

0018-9480/91/0700-1126$01.00 ©1991 IEEE

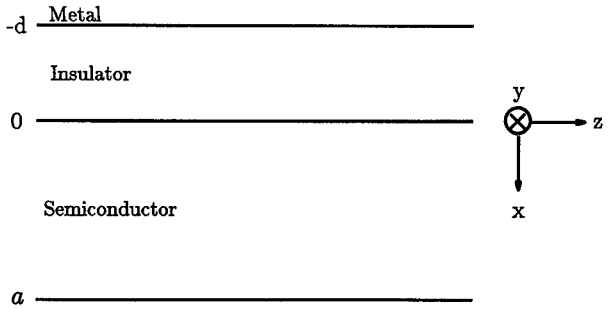

Fig. 1. The MIS structure and coordinate system employed in the analysis.

external bias. Because of their long response time, oxide charges and surface states can be ignored at microwave frequencies. The wave-guiding properties of the MIS structure are examined by assuming that a small ac signal is superimposed on a dc bias which can be adjusted to result in accumulation and depletion of the majority carrier in the region within a few Debye lengths from the interface with the dielectric.

II. Mathematical Formulation

The structure under consideration is shown in Fig. 1. The physical quantities of concern, such as field intensity, current density, and charge carrier densities, are governed by Maxwell's equations and the equations of motion for the carriers, as described in the following.

1) Maxwell's Equations:

$$\nabla \times \boldsymbol{E} = -\mu \frac{\partial \boldsymbol{H}}{\partial t} \tag{1}$$

$$\nabla \times \boldsymbol{H} = \epsilon \frac{\partial \boldsymbol{E}}{\partial t} + \boldsymbol{J} \tag{2}$$

$$\nabla \cdot \boldsymbol{E} = \frac{q}{\epsilon}(p - n + N_d - N_a) \tag{3}$$

$$\nabla \cdot \boldsymbol{H} = 0 \tag{4}$$

where $\boldsymbol{E}$ and $\boldsymbol{H}$ are the electric and magnetic fields, respectively, $\boldsymbol{J}$ is the conduction current density, and N_d and N_a are the concentrations of donor and acceptor impurities in the semiconductor, respectively.

2) Equations of Motion for Carriers:

$$\frac{\partial(n\boldsymbol{v}_n)}{\partial t} = -\frac{kT}{m_n}\nabla n - \frac{qn}{m_n}\boldsymbol{E} - \frac{n\boldsymbol{v}_n}{\tau_n} \tag{5a}$$

$$\boldsymbol{J}_n = -qn\boldsymbol{v}_n \tag{5b}$$

$$\frac{\partial(p\boldsymbol{v}_p)}{\partial t} = -\frac{kT}{m_p}\nabla p + \frac{qp}{m_p}\boldsymbol{E} - \frac{p\boldsymbol{v}_p}{\tau_p} \tag{6a}$$

$$\boldsymbol{J}_p = qp\boldsymbol{v}_p \tag{6b}$$

$$\boldsymbol{J} = \boldsymbol{J}_n + \boldsymbol{J}_p \tag{7}$$

where $\boldsymbol{v}$, m, and τ are the velocity, the effective mass, and the momentum relaxation time, respectively, of the charge carriers (n for electrons and p for holes). T is the absolute temperature and k is the Boltzmann constant.

3) Continuity Equations:

$$\nabla \cdot \boldsymbol{J}_n = q\frac{\partial n}{\partial t} + qR_n \tag{8}$$

$$\nabla \cdot \boldsymbol{J}_p = -q\frac{\partial p}{\partial t} - qR_p \tag{9}$$

where R_n and R_p are, respectively, the electron and hole net recombination rates. These rates are related to the excess carrier densities by the corresponding lifetimes, t_n and t_p, from Shockley–Read–Hall recombination statistics [17] with the assumption of small disturbance from equilibrium, single-level traps at midgap, and electrons and holes having equal capture cross sections, so that $R_n = n_a / t_n$ and $R_p = p_a / t_p$.

For an arbitrary variable $u(\boldsymbol{r}, t)$, we have

$$u(\boldsymbol{r}, t) = u_0(\boldsymbol{r}) + u_a(\boldsymbol{r})e^{j\omega t} \tag{10}$$

where $u_0(\boldsymbol{r})$ corresponds to the static component when applicable, and $u_a(\boldsymbol{r})e^{j\omega t}$ represents the dynamic (ac) part of the variable of concern. Because of the presence of the insulator, the current densities do not have a dc component. For the other variables, two sets of equations can be obtained from (1) through (10), one set for the static parts and another for the dynamic parts.

III. Method of Solution and Numerical Results

The solutions to the static set of equations can be obtained with the introduction of a scalar potential $\boldsymbol{E}_0 = -\nabla\phi$ so that the usual Boltzmann statistics for the carrier concentrations

$$n_0 = n_i e^{q(\phi - \phi_f)/kT} \quad \text{and} \quad p_0 = n_i e^{q(\phi_f - \phi)/kT}$$

follow immediately. The quasi-Fermi level, ϕ_f, can be determined from the neutrality requirement in the bulk of the semiconductor [18]. The finite difference technique and Newton's iterative procedure [19], [20] are employed to solve the resulting Poisson's equation. For the set of ac equations, we let the z dependence of all the variables have the form $e^{-\gamma z}$. The usual TE and TM classification of the propagation mode is applicable to the MIS structure, with the fundamental being a TM mode. It is of interest to note that the TE waves do not couple with the space charge because the electric field has only the y component.

By taking into consideration the boundary condition $E_{az}(-d) = 0$ on the surface of the metal, the field components in the dielectric can be obtained as

$$E_{az} = -\frac{Ak_{ci}}{\gamma}\sin k_{ci}(x + d) \qquad E_{ax} = A\cos k_{ci}(x + d)$$

$$H_{ay} = \frac{j\omega\epsilon_i A}{\gamma}\cos k_{ci}(x + d) \tag{11}$$

where $k_{ci}^2 = \omega^2\mu_0\epsilon_i + \gamma^2$ and A is an arbitrary constant depending on the magnitude of the excitation.

The field and charge carrier densities in the semiconductor layer satisfy the following set of differential equations, which are derived from (1) through (10) after linearization:

$$\frac{D_n}{\mu_n}\frac{\partial^2 n_a}{\partial x^2}+E_0\frac{\partial n_a}{\partial x}+\left[\frac{\partial E_0}{\partial x}+\gamma^2\frac{D_n}{\mu_n}-\frac{1+j\omega t_n}{\mu_{ne}t_n}-\frac{qn_0}{\epsilon_s}\right]n_a=-\frac{qn_0}{\epsilon_s}p_a-\frac{\partial n_0}{\partial x}E_{ax} \tag{12}$$

$$-\frac{D_p}{\mu_p}\frac{\partial^2 p_a}{\partial x^2}+E_0\frac{\partial p_a}{\partial x}+\left[\frac{\partial E_0}{\partial x}-\gamma^2\frac{D_p}{\mu_p}+\frac{1+j\omega t_p}{\mu_{pe}t_p}+\frac{qp_0}{\epsilon_s}\right]p_a=\frac{qp_0}{\epsilon_s}n_a-\frac{\partial p_0}{\partial x}E_{ax} \tag{13}$$

$$\frac{\partial^2 E_{az}}{\partial x^2}+k_{cs}'^2E_{az}=\frac{q\gamma}{\epsilon_s}(j\omega\mu_0\epsilon_s D_{pe}-1)p_a+\frac{q\gamma}{\epsilon_s}(1-j\omega\mu_0\epsilon_s D_{ne})n_a \tag{14}$$

and

$$E_{ax}=-\frac{\gamma}{k_{cs}^2}\frac{\partial E_{az}}{\partial x}+\frac{j\omega\mu_0}{k_{cs}^2}J_{ax} \tag{15a}$$

$$H_{ay}=-\frac{j\omega\epsilon_s}{k_{cs}^2}\frac{\partial E_{az}}{\partial x}+\frac{\gamma}{k_{cs}^2}J_{ax} \tag{15b}$$

where $k_{cs}^2=\omega^2\mu_0\epsilon_s+\gamma^2$, $k_{cs}'^2=k_{cs}^2-j\omega\mu_0\sigma_0$, and $\sigma_0=q\mu_{ne}n_0+q\mu_{pe}p_0$. The subscripts ax, ay, and az indicate the x, y, and z components of the corresponding dynamic variables, respectively, and

$$\mu_{ne}=\frac{q\tau_n}{m_n}\frac{1}{1+j\omega\tau_n}=\frac{\mu_n}{1+j\omega\tau_n}$$

$$D_{ne}=\frac{kT\tau_n}{m_n}\frac{1}{1+j\omega\tau_n}=\frac{D_n}{1+j\omega\tau_n}$$

$$\mu_{pe}=\frac{q\tau_p}{m_p}\frac{1}{1+j\omega\tau_p}=\frac{\mu_p}{1+j\omega\tau_p}$$

$$D_{pe}=\frac{kT\tau_p}{m_p}\frac{1}{1+j\omega\tau_p}=\frac{D_p}{1+j\omega\tau_p}$$

are the effective ac mobility and diffusion coefficient of the electron and the hole, respectively. Einstein's relations are satisfied by these parameters, so that

$$\frac{D_{ne}}{\mu_{ne}}=\frac{D_{pe}}{\mu_{pe}}=\frac{kT}{q}.$$

Equations (12) through (14) are the set of coupled equations for the electromagnetic field and the space charge. These equations are reduced to the wave equations for the waveguide with a uniform conductivity in the semiconductor if the ac components of the carrier densities are dropped and constant values are used for n_0 and p_0.

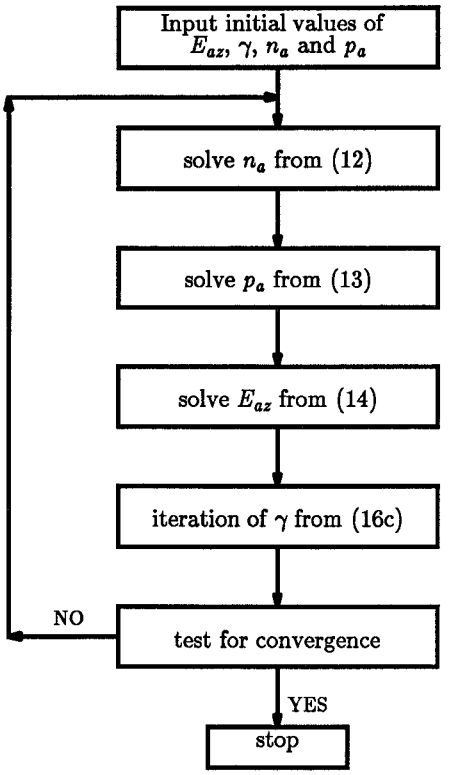

Fig. 2. Flowchart of the iterative algorithm for solving the discretized set of equations.

The boundary conditions for the variables are taken as follows:

$$E_{az}(0)=-\frac{Ak_{ci}}{\gamma}\sin k_{ci}d \tag{16a}$$

$$E_{az}(a)=0 \tag{16b}$$

$$H_{ay}(0)=\frac{j\omega\epsilon_i A}{\gamma}\cos k_{ci}d \tag{16c}$$

and

$$J_{anx}(0)=0 \tag{17a}$$

$$n_a(a)=0 \tag{17b}$$

$$J_{apx}(0)=0 \tag{17c}$$

$$p_a(a)=0 \tag{17d}$$

Equations (17a) and (17c) are obtained by observing that the normal components of the conduction currents must vanish at a dielectric–semiconductor interface. Equations (12) through (17) are a set of equations linear in the field components and dynamic variables, but nonlinear in γ. These equations can be solved by the finite difference technique. Because of the rapid variation in the variables at the surface of the semiconductor, the choice of a uniform mesh point distribution would hardly

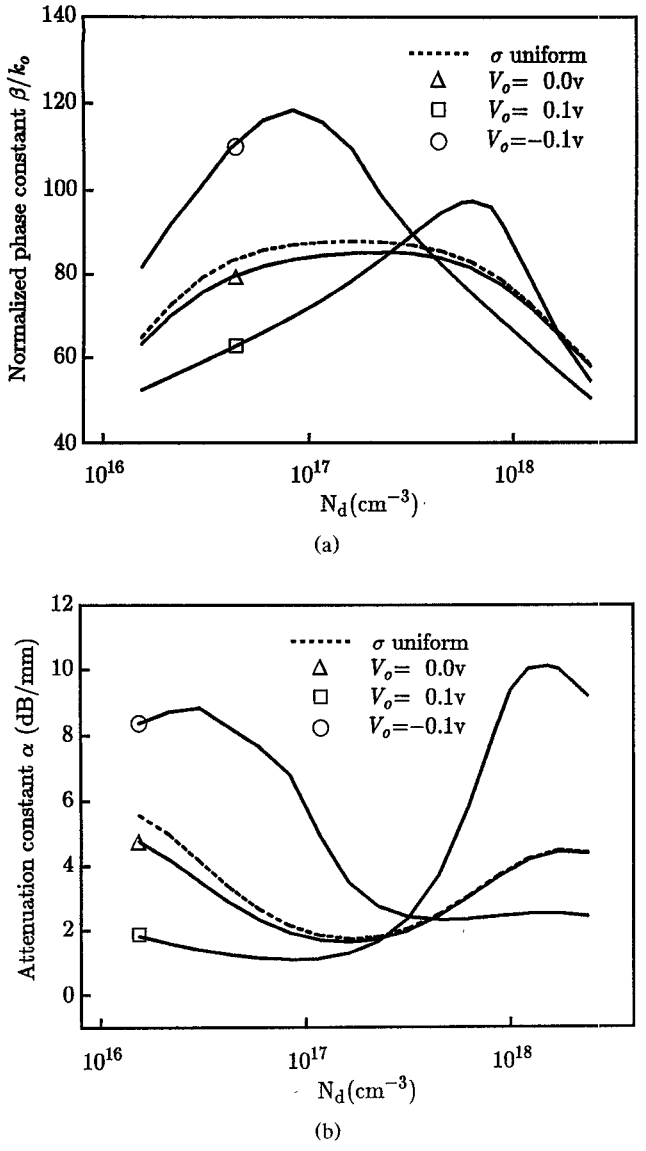

Fig. 3. (a) Normalized phase constant β/k_0 of the fundamental mode versus the concentration of donor impurity at 1 GHz. (b) Attenuation constant α of the fundamental mode versus the concentration of donor impurity at 1 GHz.

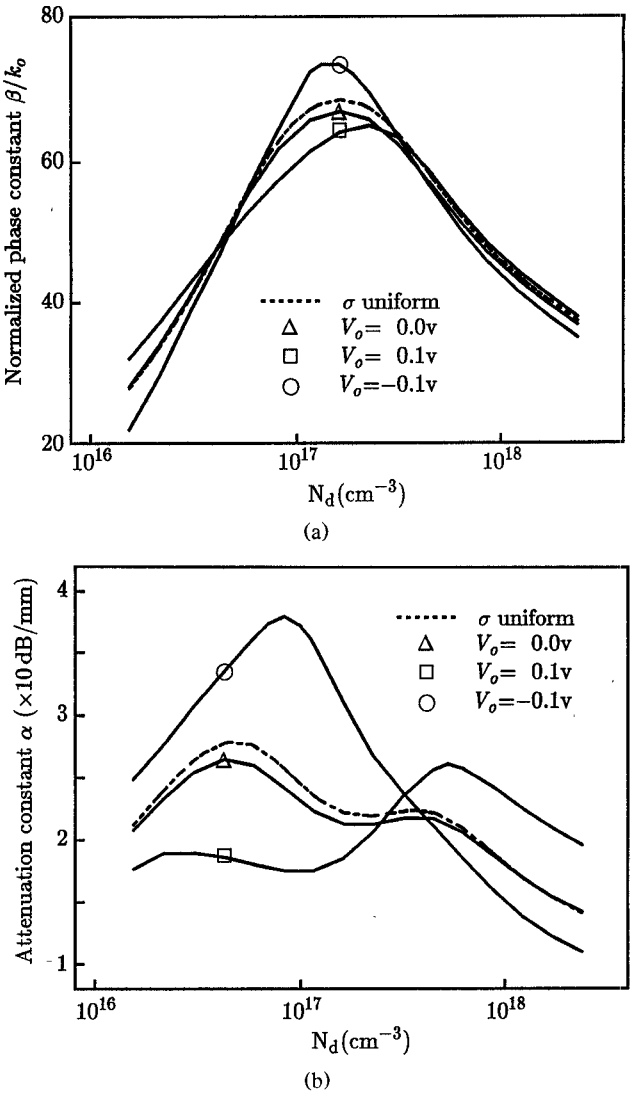

Fig. 4. (a) Normalized phase constant β/k_0 of the fundamental mode versus the concentration of donor impurity at 5 GHz. (b) Attenuation constant α of the fundamental mode versus the concentration of donor impurity at 5 GHz.

be satisfactory. In order to achieve good accuracy with a matrix of relatively small size, the mesh point distribution near the interface of the semiconductor and the insulator requires a step size much smaller than that needed in the quasi-neutral region. Since the equations are nonlinear in γ, it is basically a nonlinear system of equations. Putting γ aside, the other dynamic variables are related to each other by a system of linear equations which in principle can be solved by conventional techniques. However, because of the difference in the order of magnitude between the variables, especially for the carrier densities at different locations, standard methods for solving systems of linear algebraic equations gave solutions which were insensitive to variations in the region with low carrier concentrations, and affected the convergence in the iteration for γ. To overcome this, the algorithm described by the flowchart in Fig. 2 has been developed.

Numerical results for the fundamental mode (TM) are presented in Figs. 3 through 9. These calculations were carried out for the MIS parallel-plate waveguide assuming an insulator thickness of 0.05 μm, an n_i of 10^{10} cm^{-3}, a work function of the metal so chosen that a flat-band condition is attained in the absence of external bias, an m_n of 2.3665×10^{-31} kg, an m_p of 1.8764×10^{-31} kg, a τ_n of 2.2156×10^{-13} s, a τ_p of 5.2706×10^{-14} s, and t_n and t_p both taken to be 2.5×10^{-3} s. The value of a, the thickness of the n-type semiconductor, is chosen to be 100 μm, which is much larger than the Debye length so that the actual value has little influence on the propagation characteristics. Since the equations are linear in the field quantities, the propagation constants obtained are independent of the magnitude of the excitation. The ac components of the carrier densities, however, are dependent on the magnitude of excitation and are presented here, with A taken to be 1 V/m. It is of interest to note that

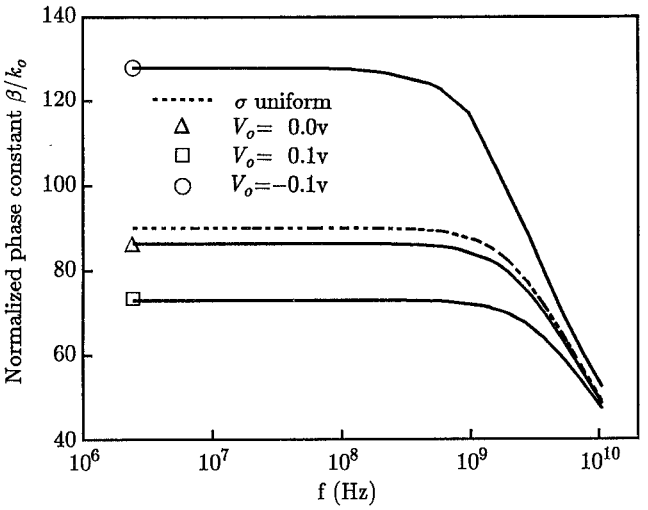

(a)

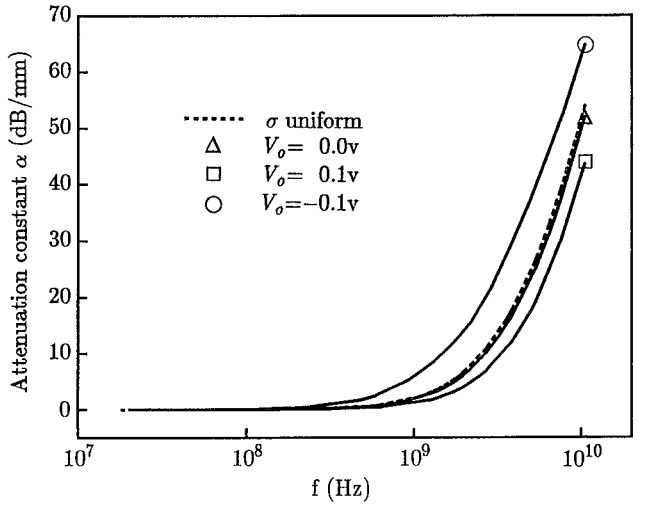

(b)

Fig. 5. (a) Normalized phase constant β/k_0 of the fundamental mode versus frequency for $N_d = 10^{17}$ cm^{-3}. (b) Attenuation constant α of the fundamental mode versus frequency for $N_d = 10^{17}$ cm^{-3}.

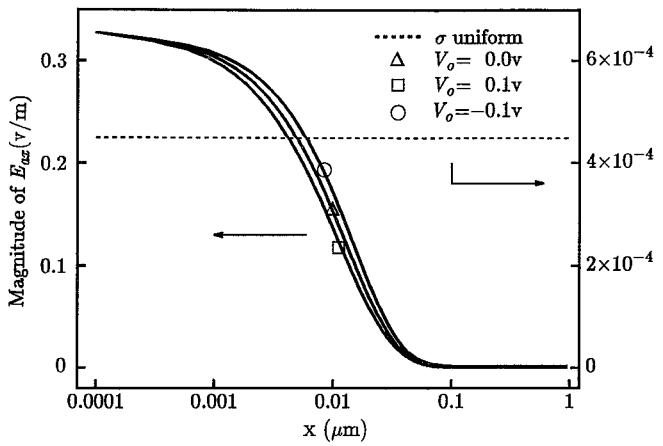

Fig. 6. Magnitude of the transverse component of the ac electric field E_{ax} in the semiconductor with $N_d = 10^{17}$ cm^{-3} at 5 GHz.

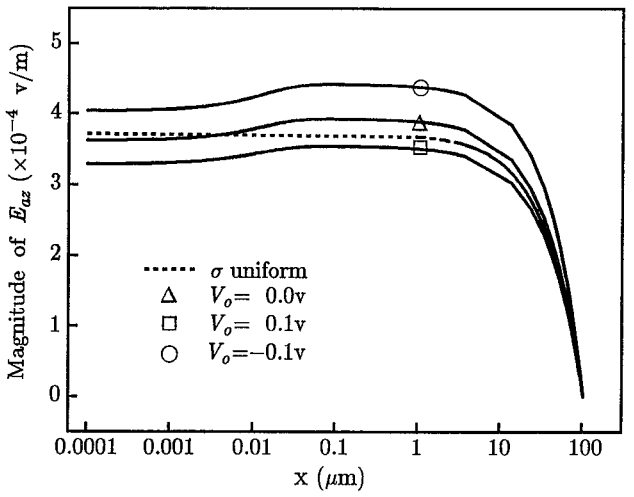

Fig. 7. Magnitude of the longitudinal component of the ac electric field E_{az} in the semiconductor with $N_d = 10^{17}$ cm^{-3} at 5 GHz.

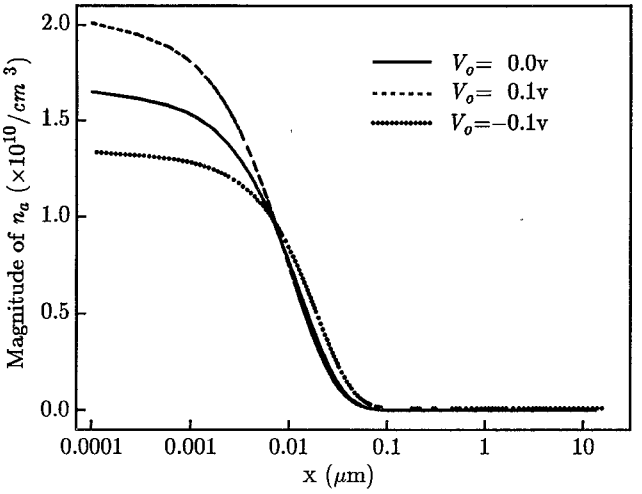

Fig. 8. Magnitude of the ac component of the electron concentration in the semiconductor with $N_d = 10^{17}$ cm^{-3} at 5 GHz.

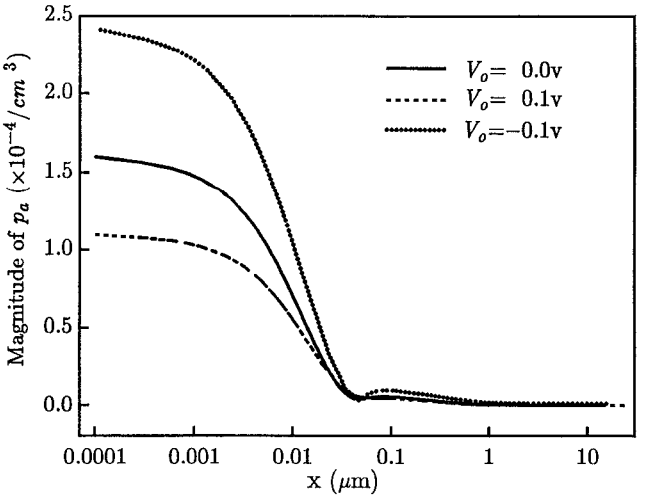

Fig. 9. Magnitude of the ac component of the hole concentration in the semiconductor with $N_d = 10^{17}$ cm^{-3} at 5 GHz.

the result on the propagation constant obtained using a uniform conductivity description closely matches that obtained using the transport-based formulation under zero bias, as shown in Figs. 3 to 5. It is also evident that carrier accumulation and depletion resulting from dc bias have significant influence on the propagation characteristics. In addition, there is a significant difference in the transverse components of the electric field, E_{ax}, obtained using the transport-based formulation for the unbiased case and that given by calculations based on uniform conductivity, as shown in Fig. 6. The screening effect of the carriers prevents the transverse component of the electric field from penetrating the semiconductor to beyond a few Debye lengths, as indicated by the solid curves. On the other hand, the dashed curve given by a uniform conductivity calculation attains a much lower value throughout the entire region of the semiconductor. The longitudinal component of the electric field, E_{az}, however, does not couple strongly with the carriers, as shown in Fig. 7. The two formulations give similar results for the unbiased case. By comparing Figs. 6, 8 and 9, one may conclude that the ac components of the charge distributions are closely related to E_{ax}, as one would expect from the screening consideration. From the presented results, a quantitative estimate of the carrier distribution as well as of their interaction with the electromagnetic wave can be made. This is achieved by treating the carrier density and the carrier velocity as individual dynamic variables.

IV. Conclusion

An analysis of the MIS parallel-plate waveguide is presented. The formulation takes into consideration the dynamics of the carriers by coupling their equations of motion to the full set of Maxwell's equations. This allows for the treatment of carrier accumulation and depletion under the influence of an external dc bias, as well as the dynamical consequence of the screening effect of the carriers. Small-signal ac solutions to the set of coupled equations were obtained numerically using an iterative algorithm. The variable-delay capability of the MIS waveguide is clearly shown by the numerical results. By comparing the electric field components with the carrier distributions, one can conclude that the penetration of the transverse component of the electric field into the semiconductor is mainly influenced by the screening effect of the carriers, whereas the longitudinal component is to a large extent governed by energy dissipation resulting from conduction current. The presented formulation and solution algorithm can be applied to other multilayer structures where wave-guiding properties are strongly influenced by carrier densities and dynamics.

References

[1] T. M. Hyltin, "Microstrip transmission on semiconductor dielectrics," *IEEE Trans. Microwave Theory Tech.*, vol. MTT-13, pp. 777–781, Nov. 1965.

[2] H. Guckel, P. A. Brennan, and I. Palócz, "A parallel-plate waveguide approach to micro-miniaturized planar transmission lines for integrated circuits," *IEEE Trans. Microwave Theory Tech.*, vol. MTT-15, pp. 468–476, Aug. 1967.

[3] H. Hasegawa, M. Furukawa, and H. Yanai, "Properties of microstrip line on Si–SiO_2 system," *IEEE Trans. Microwave Theory Tech.*, vol. MTT-19, pp. 869–881, Nov. 1971.

[4] J. M. Jaffe, "A high-frequency variable delay line," *IEEE Trans. Electron Devices*, vol. ED-19, pp. 1292–1294, Dec. 1972.

[5] D. Jäger, W. Rabus, and W. Eickhoff, "Bias-dependent small-signal parameters of Schottky contact microstrip lines," *Solid-State Electron.*, vol. 17, pp. 777–783, 1974.

[6] G. W. Hughes and R. M. White, "Microwave properties of nonlinear MIS and Schottky-barrier microstrip," *IEEE Trans. Electron Devices*, vol. ED-22, pp. 945–956, Oct. 1975.

[7] P. Kennis and L. Faucon, "Rigorous analysis of planar MIS transmission lines," *Electron. Lett.*, vol. 17, pp. 454–456, May 1981.

[8] Y. Fukuoka, Y. C. Shih, and T. Itoh, "Analysis of slow-wave coplanar waveguide for monolithic integrated circuits," *IEEE Trans. Microwave Theory Tech.*, vol. MTT-31, pp. 567–573, July 1983.

[9] R. E. Neidert and C. M. Krowne, "Voltage variable microwave phase shifter," *Electron. Lett.*, vol. 21, pp. 636–638, July 1985.

[10] C. M. Krowne, "Slow-wave propagation in two types of cylindrical waveguides loaded with a semiconductor," *IEEE Trans. Microwave Theory Tech.*, vol. MTT-33, pp. 335–339, Apr. 1985.

[11] C. Seguinot, P. Kennis, and P. Pribetich, "Performance of interconnections laid on insulating and MIS substrates," *Electron. Lett.*, vol. 22, pp. 287–289, Feb. 1986.

[12] T. C. Mu, H. Ogawa, and T. Itoh, "Characteristics of multiconductor, asymmetric, slow-wave microstrip transmission lines," *IEEE Trans. Microwave Theory Tech.*, vol. MTT-34, pp. 1471–1477, Dec. 1986.

[13] C. M. Krowne and E. J. Cukauskas, "GaAs slow-wave phase shifter characteristics at cryogenic temperatures," *IEEE Trans. Electron Devices*, vol. ED-34, pp. 124–129, Jan. 1987.

[14] Y. R. Kwon, V. M. Hietala, and K. S. Champlin, "Quasi-TEM analysis of 'slow-wave' mode propagation on coplanar microstructure MIS transmission lines," *IEEE Trans. Microwave Theory Tech.*, vol. MTT-35, pp. 545–551, June 1987.

[15] C. M. Krowne and G. B. Tait, "Propagation in layered biased semiconductor structures based on transport analysis," *IEEE Trans. Microwave Theory Tech.*, vol. 37, pp. 711–722, Apr. 1989.

[16] Y. Fukuoka, and T. Itoh, "Field analysis of a millimeter-wave GaAs double-drift IMPATT diode in the traveling-wave mode," *IEEE Trans. Microwave Theory Tech.*, vol. MTT-33, pp. 216–221, Mar. 1985.

[17] C. T. Sah, R. N. Noyce, and W. Shockley, "Carrier generation and recombination in P-N junctions and P-N junction characteristics," *Proc. IRE*, vol. 45, pp. 1228–1243, Sept. 1957.

[18] R. H. Kingston and S. F. Neustadter, "Calculation of the space charge, electric field, and free carrier concentration at the surface of a semiconductor," *J. Appl. Phys.*, vol. 26, pp. 718–720, June 1955.

[19] R. W. Klopfenstein and C. P. Wu, "Computer solution of one-dimensional Poisson's equation," *IEEE Trans. Electron Devices*, vol. ED-22, pp. 329–333, June 1975.

[20] R. C. Jaeger and F. H. Gaensslen, "Simulation of impurity freeze-out through numerical solution of Poisson's equation with application to MOS device behavior," *IEEE Trans. Electron Devices*, vol. ED-27, pp. 914–890, May 1980.

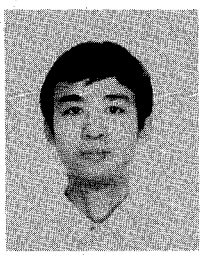

Keli Han (S'90) was born in Changsha, China, on November 9, 1959. He received the B.S. and M.S. degrees from the University of Electronic Science and Technology of China, Chengdu, China, in 1981 and 1984, respectively. He is currently working toward the Ph.D. degree in electrical engineering at the Illinois Institute of Technology, Chicago, where he is a Teaching Assistant. His research interests include electromagnetic wave propagation, semiconductor device theory, and computation methods.

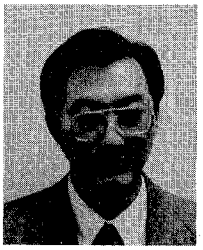

Thomas T. Y. Wong (S'74–M'80) was born in 1952. He received the B.Sc. (Eng.) degree from the University of Hong Kong in 1975 and the M.S. and Ph.D. degrees from Northwestern University in 1978 and 1980, respectively.

He was a Product Engineer at Motorola Semiconductor, Inc., from 1975 to 1976. At Northwestern University, he participated in establishing the Microwave Characterization Laboratory, where he carried out transport and dielectric studies on ionic conductors, polymers, and ceramics. He was a Research Fellow of the Materials Research Center in 1981. Since September 1981, he has been with the Illinois Institute of Technology, Chicago, where he is now Associate Professor and Director of the Graduate Program in Electrical and Computer Engineering. At IIT he has initiated research programs in transient phenomena and high-speed devices, introduced courses in electron devices, microwave theory, and quantum electronics, and developed the Microwave Electronics Laboratory.

Dr. Wong has served as Chairman (1987–1988) of the IEEE Chicago Joint Chapter of Antennas and Propagation and Microwave Theory and Techniques Societies. Currently he is Secretary of the 1992 IEEE APS/URSI/NEM Joint Symposia, to be held in Chicago.